Embedded Pin Power Reconstruction in APEC Leakage-corrected Nodal Analysis

Seongdong Jang, Yunseok Jeong, and Yonghee Kim*
Korea Advanced Institute of Science and Technology (KAIST)
291 Daehak-ro, Yuseong-gu, Daejeon, 34141, Republic of Korea
**Corresponding author: yongheekim@kaist.ac.kr*

1. Introduction

The conventional two-step method based on simplified equivalence theory is a cornerstone in modern reactor analysis [1]. As part of post-processing of the fuel assembly-wise (FA-wise) diffusion nodal analysis, a pin power reconstruction (PPR) is usually estimated by the form function (FF) method [2]. Recently, the embedded pin power reconstruction (EPPR) method was proposed [3, 4] based on the old idea of the 'embedded' PPR approach [5]. It was shown that the EPPR method can significantly enhance the accuracy of pin-wise power profiles compared to that of the conventional FF method. Moreover, the possibility of improving the EPPR accuracy was noticed when the accuracy of the diffusion nodal analysis in the conventional two-step method is improved.

The efforts to improve the accuracy of FA-wise nodal analysis appeared as a form of leakage correction by adjusting the homogenized group constants (HGCs) and equivalence group constants. The albedo-corrected parameterized equivalence constants (APEC) leakage correction method was proposed to correct flux-weighted constants (FWCs) and discontinuity factors (DFs) by taking into account actual leakage through the FA surfaces in terms of normalized leakage parameter such as current to flux ratio (CFR) [6, 7, 8, 9, 10]. Results showed that the APEC method can substantially improve the nodal accuracy in terms of the multiplication factor and RMS error in FA-wise power. In this study, the assessment of the EPPR accuracy in APEC leakage-corrected nodal expansion method (NEM) analysis is discussed by analyzing UOX-loaded SMR variant cores.

2. Embedded Pin Power Reconstruction in Two-step Nodal Analysis

The FA-wise, pin-wise lattice, and direct whole core reference calculation were conducted by DeCART2D code [11]. The diffusion NEM analysis was performed by in-house nodal code, which solves the two-group diffusion equation as shown in Eq. (1).

$$\nabla\cdot\vec{J}_g(r)+\Sigma_{r,g}(r)\phi_g(r)-\frac{\chi_g}{k_{eff}}\sum_{g=1}^{2}\nu\Sigma_{f,g}(r)\phi_g(r)+\sum_{g'=1,g'\neq g}^{2}\Sigma_{s,g'\to g}(r)\phi_{g'}(r)=0,\quad g=1,2. \tag{1}$$

2.1 APEC Leakage-corrected two-step nodal analysis

The APEC leakage correction was implemented by predetermined APEC XS and DF functions obtained by additional color-set calculation. The APEC XS and DF functions were defined as shown in Ref. [8], which aimed to correct XSs and DFs in 1x1 NEM analysis. In this study, the corrected XSs and DFs were obtained by APEC-corrected 1x1 NEM analysis and then were applied to 2x2 NEM analysis for determining the boundary condition of EPPR.

2.2 Embedded Pin Power Reconstruction

The main principle of the EPPR method is to solve a fixed boundary source problem in the expanded domain of interested FA as shown in Fig.1. The EPPR-H denoted that the domain was expanded to half of FA. In the EPPR-H, the incoming partial currents were obtained by 2x2 nodal analysis as shown in Eq. (2).

$$\vec{J}_g^{in}(r)=\frac{\phi_g(r)}{4}-\frac{\vec{J}_g(r)}{2}=f_{BC}(r),\qquad r\in\Gamma \text{ and } g=1,2. \tag{2}$$

Using HGCs and pin-wise DFs (PDFs) generated by pin-wise lattice calculation, the standard 2-node CMFD equation based on the fine-mesh NEM was constructed as shown in Eq. (3).

$$(A-\frac{1}{k_{eff}}F)\Phi=S_{BC}, \tag{3}$$

where, A, Φ, F, S_{BC} denoted CMFD matrix, pin-wise flux vector, fission matrix and vector for the boundary source, respectively. The coupled two-group equation was directly solved by BiCGstab method [12].

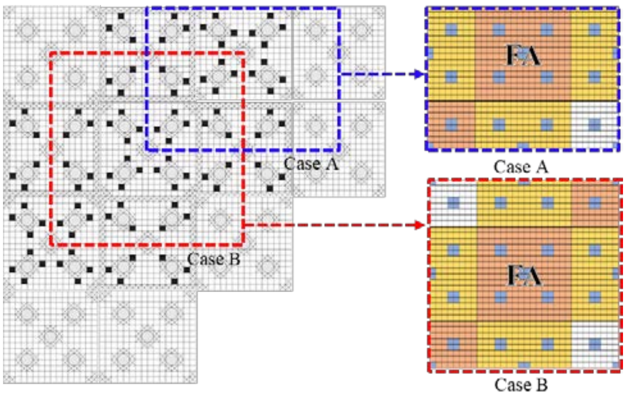

Fig. 1. Configuration of EPPR-H

3. Numerical Results

3.1 UOX-loaded SMR Benchmark Problem

The UOX-loaded SMR and variant cores were set up as the benchmark problem, which consist of 16x16 FA as shown in Fig. 2 and 3.

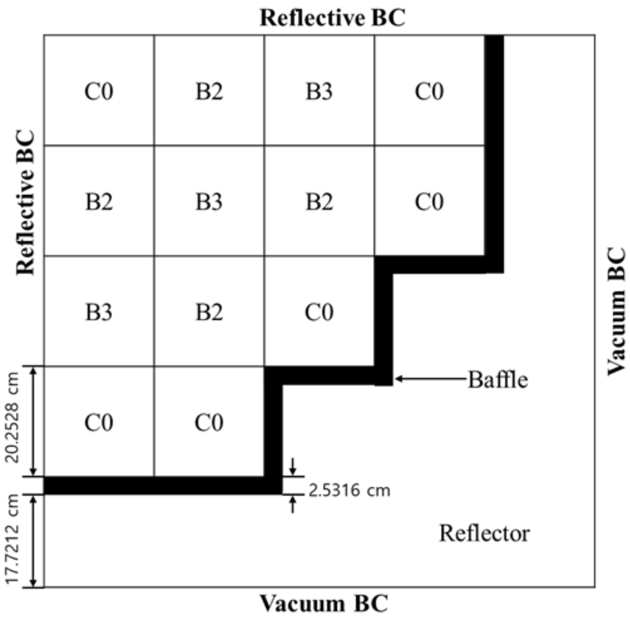

Fig. 2. Core configuration of UOX-loaded SMR.

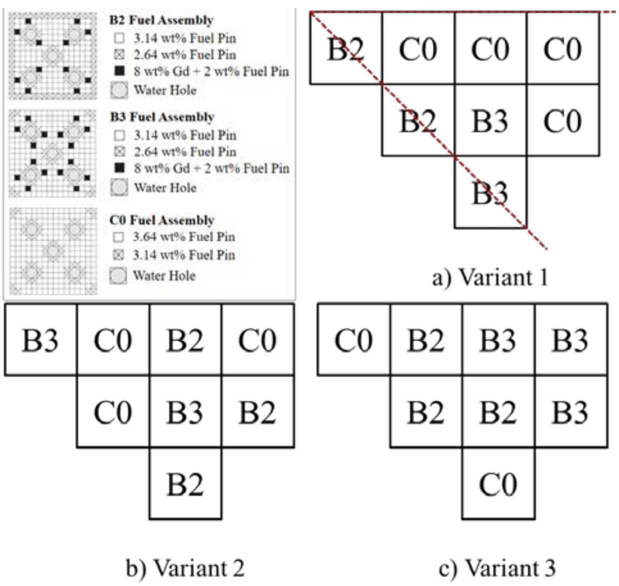

Fig. 3. Configuration of fuel assembly and variant cores.

3.2 Results of APEC leakage-corrected nodal analysis

The additional color-set configuration and list for APEC functions were depicted in Fig.4 and Table I. Results show that the APEC leakage correction can improve the nodal solution as shown in Table II and Fig.5. It should be noted that the nodal analysis based on GET cannot be achieved reference solution because 2x2 nodal analysis was conducted based on 1x1 HGCs and DFs.

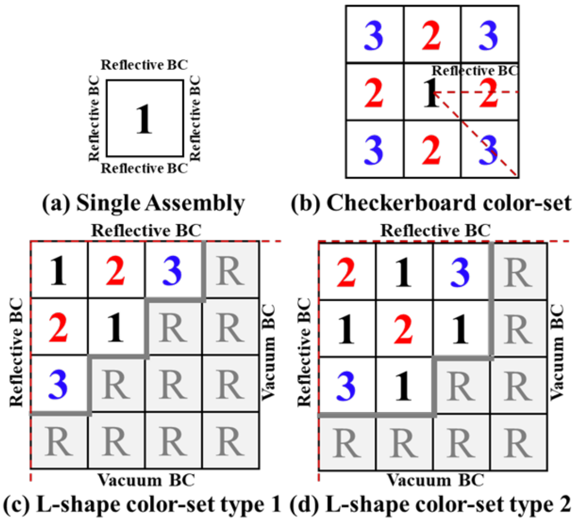

Fig. 4. Color-set models for constructing APEC functions.

Table I: List of Color-set models

Color-set Model	Combination of FAs
Checkerboard	(B2,B3,C0), (B3,C0,B2), (C0,B3,B2)
L-Shape Type1	(B2,B3,C0), (B2,C0,B3), (B3,B2,C0), (B3,C0,B2), (C0,B2,B3), (C0,B3,B2)
L-Shape Type2	(B2,B3,C0), (B2,C0,B3), (B3,C0,B2), (B3,B2,C0), (C0,B2,B3), (C0,B3,B2), (B2,B3,B2), (C0,B2,C0), (B3,C0,B3)

Table II: Results of 2x2 NEM Analysis

HGCs	k_{eff}	$\Delta\rho$ (pcm)	RMS[a] (%)	Min.[b] (%)	Max.[c] (%)
Ref.	1.074921	*UOX-loaded SMR*			
GET[d]	1.074718	-17.58	0.32	-0.66	0.28
SET[e]	1.076350	123.47	0.91	-1.21	1.28
APEC[f]	1.074721	-17.31	0.49	-0.83	0.83
Ref.	1.127021	*Variant 1*			
GET	1.126826	-15.35	0.10	-0.17	0.15
SET	1.128441	111.65	0.55	-0.96	0.87
APEC	1.126932	-6.98	0.38	-0.35	0.65
Ref.	1.100274	*Variant 2*			
GET	1.100196	-6.48	0.09	-0.13	0.22
SET	1.101763	122.82	0.60	-0.99	0.50
APEC	1.100554	23.10	0.46	-0.97	0.68
Ref.	1.07113	*Variant 3*			
GET	1.070981	-13.00	0.26	-0.50	0.19
SET	1.072526	121.48	0.75	-1.15	1.02
APEC	1.071194	5.62	0.48	-0.84	0.63

a: Root Mean Square Error of Assembly Power (%),
b: Minimum Relative Error in Assembly power (%),
c: Maximum Relative Error in Assembly power (%),
d: Generalized Equivalence Theory (GET: Ref. XS | Ref. DF),
e: Simplified Equivalence Theory (SET: FWC | ADF),
f: APEC Leakage Correction (APEC: APEC XS | APEC DF).

3.31	**1.57**	**0.81**	**0.61**
0.12	0.28	0.06	-0.35
0.34	-0.41	-1.05	0.89
-0.26	0.83	-0.32	-0.83
	1.04	**0.66**	**0.43**
	-0.03	-0.66	-0.06
	-1.21	0.24	1.28
	0.02	-0.01	-0.20
		0.49	
		-0.05	
		1.27	
		-0.06	

Ref. FA power
%Error of GET
%Error of SET
%Error of APEC

a) UOX-loaded core

1.33	**1.76**	**1.47**	**0.82**
0.14	0.06	-0.07	-0.06
-0.45	0.09	0.21	0.29
0.51	-0.13	-0.35	-0.21
	1.03	**0.67**	**0.47**
	0.11	-0.17	-0.03
	-0.33	-0.96	0.87
	0.64	-0.11	0.65
		0.29	
		0.15	
		-0.05	
		0.06	

Ref. FA power
%Error of GET
%Error of SET
%Error of APEC

b) Variant 1

1.55	**2.05**	**1.02**	**0.61**
0.01	0.03	-0.13	0.08
-0.98	0.38	-0.17	0.50
-0.20	-0.05	0.23	-0.97
	1.72	**0.72**	**0.29**
	0.04	-0.07	-0.05
	0.40	-0.99	0.49
	0.40	0.17	0.16
		0.35	
		0.22	
		0.46	
		0.68	

Ref. FA power
%Error of GET
%Error of SET
%Error of APEC

c) Variant 2

3.92	**1.81**	**0.77**	**0.28**
-0.01	0.19	0.18	-0.33
0.79	-0.13	-1.15	-1.08
-0.55	0.63	-0.05	-0.84
	1.22	**0.63**	**0.21**
	-0.09	-0.50	0.03
	-0.25	-0.16	-0.47
	0.43	0.04	-0.42
		0.46	
		-0.03	
		1.02	
		0.04	

Ref. FA power
%Error of GET
%Error of SET
%Error of APEC

d) Variant 3

Fig. 5. Reference FA power distribution and %error of nodal analysis

3.3 Results of Pin Power Reconstruction

-3.51 (0.96)	4.35 (1.03)	3.25 (1.24)	3.48 (1.54)
-0.82 (0.32)	1.16 (0.38)	1.41 (0.51)	-1.75 (0.65)
0.62 (0.38)	-0.93 (0.46)	-1.73 (1.07)	1.78 (1.01)
-1.18 (0.43)	1.61 (0.85)	-0.83 (0.44)	-2.22 (1.01)
	-2.56 (1.27)	4.54 (1.00)	-31.50 (3.75)
	0.94 (0.32)	-1.53 (0.71)	-1.49 (0.64)
	-1.48 (1.18)	1.31 (0.51)	2.42 (1.38)
	0.89 (0.28)	0.91 (0.33)	-1.53 (0.62)
		-30.52 (3.75)	
		1.54 (0.59)	
		2.66 (1.38)	
		1.36 (0.59)	

FF-based PPR
EPPR-H with GET
EPPR-H with SET
EPPR-H with APEC

*Format: Max (RMS)

a) UOX-loaded core

3.83 (1.04)	-3.83 (0.86)	-3.58 (0.69)	-3.94 (1.32)
0.88 (0.27)	-0.83 (0.31)	-1.00 (0.25)	-1.51 (0.45)
-0.72 (0.50)	-0.59 (0.22)	0.59 (0.27)	-1.29 (0.52)
1.24 (0.58)	-0.90 (0.29)	-1.15 (0.41)	-1.67 (0.51)
	4.03 (1.13)	-3.93 (1.45)	-33.70 (3.79)
	0.84 (0.28)	1.23 (0.52)	-1.69 (0.63)
	-0.80 (0.41)	-1.76 (0.96)	1.92 (0.99)
	1.41 (0.71)	1.26 (0.46)	1.64 (0.85)
		-26.15 (3.17)	
		3.29 (0.78)	
		2.92 (0.69)	
		3.03 (0.73)	

FF-based PPR
EPPR-H with GET
EPPR-H with SET
EPPR-H with APEC

*Format: Max (RMS)

b) Variant 1

-3.50 (1.30)	-3.52 (0.95)	4.31 (1.06)	-3.65 (1.55)
1.01 (0.26)	-1.14 (0.37)	-0.57 (0.29)	-1.29 (0.52)
-1.29 (0.98)	0.65 (0.47)	-0.66 (0.32)	1.36 (0.69)
0.76 (0.30)	-1.16 (0.36)	0.94 (0.35)	-2.37 (1.13)
	-3.36 (0.97)	-3.83 (1.45)	-33.62 (3.80)
	-0.97 (0.28)	0.92 (0.39)	1.99 (0.67)
	0.76 (0.43)	-1.50 (0.99)	2.67 (0.81)
	0.72 (0.44)	1.25 (0.42)	2.23 (0.62)
		-33.61 (3.70)	
		2.36 (0.61)	
		2.84 (0.80)	
		2.75 (0.91)	

FF-based PPR
EPPR-H with GET
EPPR-H with SET
EPPR-H with APEC

*Format: Max (RMS)

c) Variant 2

-3.13 (1.18)	4.76 (1.03)	-3.24 (1.34)	-5.74 (1.61)
-1.04 (0.33)	1.13 (0.37)	0.85 (0.29)	-1.68 (0.49)
1.04 (0.79)	0.69 (0.30)	-1.49 (1.12)	-2.49 (1.05)
-1.49 (0.66)	1.43 (0.66)	0.67 (0.19)	-2.20 (0.83)
	-2.13 (0.66)	4.27 (0.95)	-28.13 (3.39)
	-0.48 (0.23)	-1.07 (0.50)	2.64 (0.66)
	-0.55 (0.29)	0.96 (0.34)	2.00 (0.75)
	0.80 (0.43)	1.16 (0.34)	2.05 (0.71)
		-33.29 (3.84)	
		-1.42 (0.62)	
		2.00 (1.05)	
		-1.39 (0.61)	

FF-based PPR
EPPR-H with GET
EPPR-H with SET
EPPR-H with APEC

*Format: Max (RMS)

d) Variant 3

Fig. 6. Reconstructed pin power %error

The maximum and RMS %error of the reconstructed pin power distribution in FA were shown in Fig. 6. Results show that the EPPR method can substantially improve the accuracy of the reconstructed pin power in the case of EPPR-H with GET compared to that of the conventional FF method. It can be comprehended as the effect of reflecting the neighboring effect by expanding the domain of the fixed boundary source problem can improve the accuracy at the interface region of the FA. Nevertheless, the higher error of maximum and RMS tended to be observed at the peripheral FA region, which was bordered to baffle-reflector region. It was noteworthy that the improvement of the EPPR accuracy could be enhanced as long as the equivalence is achieved by introducing the exact 2x2 DFs [13]. In the case of EPPR-H with SET, the tendency of the reconstructed pin power maximum and RMS %error was totally depending on the accuracy of FA-wise power distribution of the diffusion nodal analysis by 2x2 NEM. I.e., the higher the %error occurred in FA-wise power of nodal analysis, the higher %error was observed in pin-wise reconstructed power of EPPR-H.

Similarly, the accuracy of the reconstructed pin power tended to be depending on the accuracy of the FA-wise power in the case of APEC leakage-corrected nodal analysis. In other words, the EPPR-H accuracy can be improved as much as the enhancement of the nodal accuracy by APEC leakage correction. The performance of the APEC leakage correction was significant in terms of RMS error in the FA as shown in Table II. It was indicated that the overall performance of EPPR-H with APEC can be improved compared to that of EPPR-H with SET.

4. Conclusions

The EPPR-H pin-power reconstruction in APEC-corrected nodal analysis has been performed based on 2x2 NEM analysis. It is demonstrated that the EPPR-H with APEC improves reconstructed pin-wise power profile due to improvement of the nodal accuracy by the APEC leakage correction. It is expected that it may be possible to further improve the performance of the EPPR-H with improved nodal equivalence in the APEC-based nodal analysis and the proposed reconstruction method can be a new framework for the 2-step nuclear reactor core design and analysis.

ACKNOWLEDGEMENTS

This work was supported by the National Research Foundation of Korea (NRF) Grant funded by the Korean Government (MSIP) (NRF-2016R1A5A1013919)

REFERENCES

[1] K. Smith, “Assembly Homogenization Techniques for Light Water Reactor Analysis,” Prog. in Nucl. Energy, 17, 3, 303 (1986)

[2] J. M. NOH and N. Z. Cho, “A New Approach of Analytic Basis Function Expansion to Neutron Diffusion Nodal Calculation”, Nuclear Science and Engineering, Vol. 116 (3), p. 165-180, 1994

[3] H. Yu, S. Jang, and Y. Kim, “Pin Power Reconstruction with Leakage-corrected Embedded Calculation in PWRs”, Transactions of the Korean Nuclear Society Virtual Spring Meeting, July 9-10, 2020.

[4] H. Yu, S. Jang and Y. Kim, “A New Embedded Analysis with Pinwise Discontinuity Factors for Pin Power Reconstruction,” Nucl. Sci. Eng., published online, 2020.

[5] A. JONSSON and R. REC, “Nodal Imbedded Calculation for the Retrieval of Local Power Peaking from Coarse Mesh Reactor Analysis”, International Topical Meeting on Advances in Mathematical Methods for the Solution of Nuclear Engineering Problems, Vol. 2, p.23, Munich, 27-29 April, 1981

[6] W. Kim, K. Lee and Y. Kim, “Functionalization of the Discontinuity Factor in the Albedo-corrected Parameterized Equivalence Constants (APEC) Method,” Nucl. Sci. Eng., 192, 1 (2018).

[7] K. Lee, W. Kim and Y. Kim, “Improved Nodal Equivalence with Leakage-corrected Cross Sections and Discontinuity Factors for PWR Depletion Analysis,” Nucl. Eng. Tech., 51, 5, (2019).

[8] S. Jang, and Y. Kim “Improved Discontinuity Factor Modeling for the in-situ APEC Leakage Correction in Nodal Analysis,” Transactions of ANS Winter, November 17-21, Washington, D.C., 2019

[9] S. Jang, K. Lee, and Y. Kim, “APEC-corrected NEM Analysis of the VERA core”, Proceedings of Reactor Physics Asia conference, Osaka, Dec. 02-03, 2019..

[10] S. Jang, and Y. Kim, “A Study on APEC-Corrected Macroscopic Depletion in 2-D Nodal Analysis”, Transactions of the Korean Nuclear Society Virtual Winter Meeting, December 17-18, 2020.

[11] J. Y. Cho, et al., “DeCART2D v1.0 Methodology Manual,” KAERI/TR-5283/2013, Korea Atomic Energy Research Institute (2013).

[12] G. L. G. Sleijpen and D. R. Fokkema, "BiCGstab(*l*) for linear equations involving unsymmetric matrices with complex spectrums," *Electronic Transactions on Numerical Analysis*, Vol. 1, p. 11-32, 1993

[13] HyeonTae Kim, Woosong Kim, and Yonghee Kim, “Generation of Exact Discontinuity Factors for NEM Calculations with Two-by-Two Division per Fuel Assembly”, Nuclear Science and Engineering, Vol. 193:5, pp. 441-452, May 2019.